Cement & Concrete Composites 32 (2010) 801–809

Contents lists available at ScienceDirect

Cement & Concrete Composites

journal homepage: www.elsevier.com/locate/cemconcomp

Behaviour of Strain-hardening Cement-based Composites (SHCC) under monotonic and cyclic tensile loading
Part 1 – Experimental investigations

Petr Jun, Viktor Mechtcherine *

Institute of Construction Materials, TU Dresden, D-01062 Dresden, Germany

ARTICLE INFO

Article history:
Available online 11 August 2010

Keywords:
SHCC
Cyclic behaviour
Uniaxial tension test
Fibre pullout test
Microstructure

ABSTRACT

This first part of the project at hand presents the results of experiments performed on a Strain-hardening Cement-based Composite (SHCC) in order to investigate the specific behaviour of such materials under monotonic and cyclic tensile loading. The testing programme included uniaxial tension tests on dumbbell specimens, tension tests on single fibres, single-fibre pullout tests, and optical investigations. All mechanical tests were performed under deformation-controlled loading regime. Optical investigations of the SHCC microstructure provided detailed insights into the failure mechanisms observed in the mechanical tests. The results obtained can serve as a reliable basis for the development of corresponding constitutive relationships relevant to SHCC. Since the modelling to be presented in the second part of this paper is based on a multi-scale approach, the experimental results are discussed in particular with respect to the identification and description of the determinant physical phenomena influencing material performance at different levels of observation.

1. Introduction

This paper addresses the Strain-hardening Cement-based Composites (SHCC) which exhibit strain-hardening, quasi-ductile behaviour due to the bridging of fine multiple cracks by short, well-distributed fibres. The favourable mechanical properties of this material offer many possible applications in new and old structures as well as in the strengthening and repair of structural elements made of reinforced concrete or other traditional materials [1,2].

The characteristic behaviour of SHCC under monotonic tensile loading is shown in Fig. 1 and can be described as follows: Microscopic defects trigger the formation of matrix cracks at so-called first-crack stress σ_1. As the first crack forms, the fibres bridge the crack, transmitting tensile stresses across the crack surfaces. The applied load must be increased in order to force further crack formation. This leads to the subsequent development of another crack at the second weakest cross-section. The scenario then repeats itself, resulting in a set of almost uniformly distributed cracks. The strain capacity is reached at the maximum load (tensile strength f_t) when the localisation of the failure occurs, namely when one main crack develops. Due to a moderate opening of a large number of fine cracks, a strain capacity of several percent can be observed.

The behaviour of SHCC under tension brought about by monotonic, quasi-static loading has been studied intensively during the last few years; see, for example, Mechtcherine [3]. However, in practice the majority of concrete structures are exposed to more or less severe cyclic loadings such as traffic loads, temperature changes, wind gusts, sea waves in some cases, vibrations due to the operation of machinery, or in extreme circumstances earthquake. Appropriately enough, a thoroughgoing understanding of the behaviour of SHCC under fatigue is indispensable to the safe and economical design of structural members and building components for which such materials might be used.

As yet only a few investigations of SHCC behaviour under cyclic loading have been performed. Fukuyama et al. [4] investigated the cyclic tension–compression behaviour of two SHCC materials, which possessed a strain capacity of 0.5% and 1.0%, respectively. Only about five cycles were needed until the strain capacity was exhausted, while the cyclic tension response accurately reflected the corresponding curve obtained from a monotonic tension test. In contrast, Douglas and Billington [5] found that the envelope of the stress–strain curve from the cyclic tests lay below the relationship measured in the monotonic regime. The difference was particularly pronounced in the experiments with high strain rates. The SHCC investigated showed a strain capacity of approximately 0.5% when subjected to monotonic, quasi-static loading.

Mechtcherine and Jun [6] investigated SHCC with a strain capacity clearly higher than 2%. Different loading routines were applied: deformation-controlled monotonic and cyclic tests as well as load-controlled cyclic and creep tests. In addition, the effects of specimen size and curing conditions were investigated.

* Corresponding author. Tel.: +49 351 463 35 920; fax: +49 351 463 37 268.
E-mail address: mechtcherine@tu-dresden.de (V. Mechtcherine).

0958-9465/$ - see front matter © 2010 Elsevier Ltd. All rights reserved.
doi:10.1016/j.cemconcomp.2010.07.019

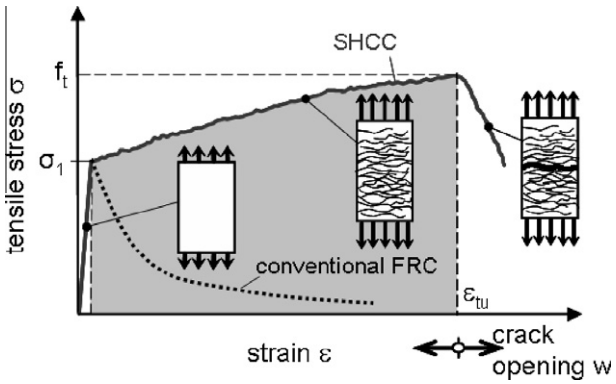

Fig. 1. Typical stress–strain response and crack pattern of SHCC specimens under monotonic tensile loading.

Simultaneously Mechtcherine [3] discussed the appropriateness of different testing techniques for uniaxial tension experiments. Furthermore, a series of fibre pullout tests was performed by Jun and Mechtcherine [7,8] in order to investigate the characteristic material behaviour on this level of observation and to establish the accurate testing technique. Based on this information, the most appropriate testing procedures were accepted as the basis of further experimental investigations.

This paper gives an overview of the experimental results obtained in uniaxial monotonic and cyclic tension tests on SHCC. In order to understand the specific material behaviour of SHCC better, single-fibre pullout tests and single fibre tension tests under monotonic and cyclic loading as well as the accompanying optical investigations were performed additionally. The results obtained can serve as a general basis for describing and explaining the mechanical performance of SHCC. The discussion of the experimental findings is conducted with special regard to the development of a multi-scale material model for SHCC under monotonic and cyclic tensile loading (this model is introduced in the second part of this paper). The major feature and advantage of such a multi-scale modelling approach is in establishing a link between basic physical mechanisms acting at the micro-level and material response observed at the macro-level. The model should not only provide a physically sound basis for deriving constitutive relations, but should also enable a comprehensive analysis of the material behaviour leading to more purposeful material design. Particular attention during the evaluation of the experimental results is therefore paid to the various specific phenomena observed on different scales of observation.

2. Material under investigation

SHCC, unlike common, fibre-reinforced concrete, is a micromechanically designed material. One approach to such material design was developed by Li [9]. Material composition used in this investigation was developed on the basis of this particular approach by Mechtcherine and Schulze [10,11]. The material chosen showed stable strain-hardening behaviour in earlier studies by the authors. With regard to its mechanical performance under monotonic tensile loading, it can be considered to be representative for SHCC.

Table 1 lays out the mix components of the investigated SHCC and their mass proportions. A mix containing a combination of Portland cement 42.5R HS and fly ash was utilized as binder. The high content of fly ash was found to be favourable for various reasons: improvement in the rheological behaviour of the fresh mix, reduction in the cement content required, and, most importantly, for inducing micro-defects to trigger the formation of numerous, well-distributed micro-cracks which foster the multiple cracking necessary to the quasi-ductile response of SHCC (due to high percentage of fly ash the larger particles are not "consumed" by the pozzolanic reaction and so remain as round inclusions in the cement paste microstructure). The fine aggregate was uniformly graded quartz sand with particle sizes of 0.06–0.20 mm. The limitation of the aggregate size served to achieve a possibly homogenous distribution of fibre over the matrix. Furthermore, polyvinyl alcohol (PVA) fibres, 2.25% of the total mix by volume, 12 mm in length, diameter of 40 μm and with a density of 1300 kg/m^3, were used. A superplasticiser (SP) and a viscosity agent (VA) were added to the mix in order to adjust its rheological properties.

Table 1
SHCC composition – mass proportions of the mix components.

Cement	Fly ash	Quartz sand	Water	SP	VA	PVA fibres
1.00	2.33	1.67	1.04	0.05	0.01	0.09

The average characteristics of this material under compression are a compressive strength of 33.7 MPa (standard deviation of 3.9 MPa), and a strain at maximum load of 0.72% (standard deviation of 0.07%). These values were derived from 12 displacement-controlled tests on cubes with a side length of 100 mm. The displacement rate used for testing was 0.01 mm/s.

3. Uniaxial tension tests

3.1. Specimen geometry, casting, curing, experimental setup

Based on the findings of previous investigations [10,11], unnotched, dumbbell shaped prisms were chosen as specimens for this study. Such prisms had a cross-section of 24 mm × 40 mm. The gauge length was 100 mm. Fig. 2a gives further geometric data for the specimens and shows the test setup.

All specimens were cast horizontally in metal forms. The moulds were stored 2 days in a climatic box (T = 25 °C, RH = 65%). Investigations on material shrinkage indicated that the development of shrinkage deformation in early age was insignificant and therefore did not induce cracking of the composite while being stored in the moulds. After de-moulding, the specimens were wrapped in a plastic foil and stored until testing at the room temperature. All specimens were tested at an SHCC age of 28–32 days.

The uniaxial tension tests were performed with non-rotatable boundaries. The deformations were measured by means of two LVDTs fixed to the specimen as displayed in Fig. 2b. The specimen surfaces were covered with thin, brittle white paint in order to facilitate monitoring of the crack's development.

3.2. Testing procedure

Two types of experiment were performed with regard to the loading procedure: (a) monotonic, deformation-controlled tests and (b) cyclic, deformation-controlled tests. The deformation rate was always 0.01 mm/s, which corresponded to a strain rate of 10^{-4} 1/s. For the cyclic tests, the increase of the total deformation within the measuring length was given by the deformation increment $\Delta\delta$, which was chosen to be 0.1 mm (this corresponds to a strain increment of 0.1%). The increment was held constant from cycle to cycle. When the preset value $\Delta\delta$ in the following cycle was reached, the specimen was unloaded until the lower reversal point δ_{min} was attained. The lower reversal point δ_{min} was defined as a function of the lower load level P_{min} = const = 0 N. Fig. 3 gives schematic description of the loading regimes used.

3.3. Results of the tension tests on SHCC specimens

Fig. 4 shows the representative results of the deformation-controlled monotonic and cyclic testing. The characteristic behaviour

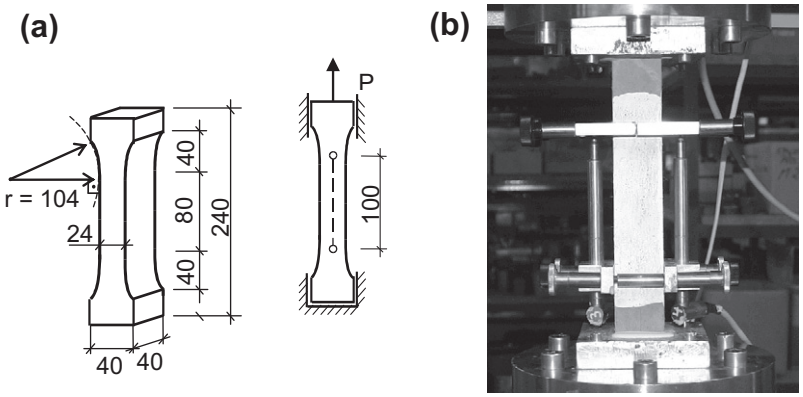

Fig. 2. Uniaxial tension tests: (a) geometry of the specimens (geometrical data is given in mm), and (b) test setup used.

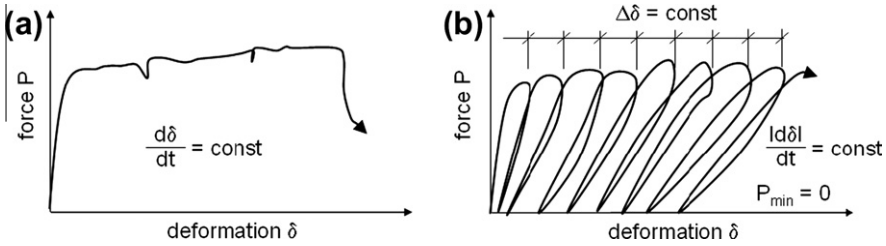

Fig. 3. Schematic description of loading regimes: (a) monotonic, and (b) cyclic.

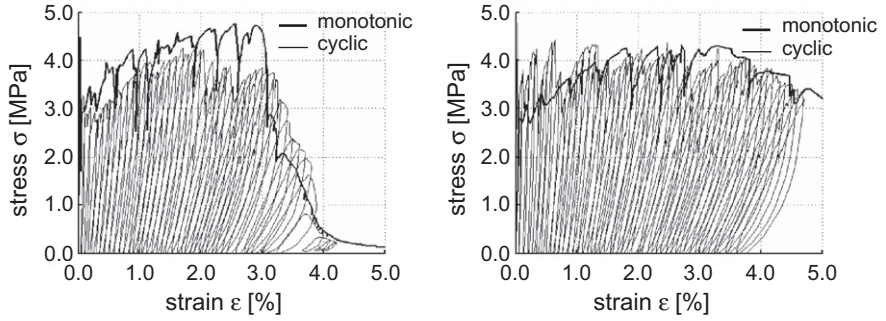

Fig. 4. Representative results from monotonic and cyclic tension tests.

of the SHCC under investigation when subjected to deformation-controlled, monotonic tensile loading can be described as follows. Before the first cracking, a linear elastic response in the composite can be observed. By definition, at first-crack stress the first crack occurs. Since the carrying capacity of fibres bridging this crack is higher than the cracking stress of the next weakest cross-section, the load can be increased further, and the second crack, third crack, and so on develop. The overall material response is characterised by strain-hardening behaviour. The progressive multiple cracking carries on until the load carrying capacity of the weakest crack is reached (i.e. the load carrying capacity of the fibres crossing this crack). When this occurs, the failure localises itself into this weakest link and the material shows a softening behaviour.

The tensile behaviour of SHCC is further characterised by sudden drops in stress due to the opening of new cracks. Before the tensile stress is fully "taken over" by bridging fibres, the crack needs to open to some extent. Due to this opening, as well as due to the applied deformation control regime, the rest of the specimen relaxes in part. Such pronounced drops were not observed in investigations [10,11] despite the use of the same material. The reason why the performance of the actual SHCC is slightly different could be related to some minor changes in the quality of the raw materials. SHCC is generally sensitive to this. However, the drop due to crack formation can be explained, possibly at least in part, by the changes of the testing machine and in the test control as well; the displacement of the machine crosshead was used in the studies [10,11]. The machine used in this investigation is characterised by a deformation-controlled regime which can tend somewhat to the over-regulation of the machine. The unsteadiness of the curves hampered to some degree the evaluation of the results but did not seem to affect otherwise the information obtained from the experiments.

A comparison of the monotonic curves with those obtained from the tests using the cyclic loading regime shows that nearly no effect of the given, relatively moderate number of loading cycles on the shape of the stress–strain diagram can be observed when considering only the envelope curves. The lack of a pronounced distinction in the envelope curves naturally results in only minor differences in the average values of the stress at first cracking σ_1, tensile strength f_t as well as the strain capacity ε_{tu} for these two different loading regimes; see Table 2. The results obtained under

Table 2
Statistical evaluation of the mechanical performance of the investigated SHCC for two loading regimes.

Type of loading	Number of cycles N (−)	Stress at first cracking σ_1 (MPa)	Tensile strength f_t (MPa)	Strain capacity ε_{tu} (%)
	Average value (standard deviation)			
Five specimens per loading type				
Monotonic	1	3.6 (0.7)	4.7 (0.3)	2.5 (0.8)
Cyclic	24 (6)	3.9 (0.7)	4.3 (0.1)	2.4 (0.6)

Table 3
Change of SHCC stiffness with increasing induced strain as observed in deformation-controlled cyclic tests.

Strain under load	Secant modulus E (MPa)
	Average value (standard deviation)
0.5%	2040 (310)
1.0%	1430 (270)
2.0%	800 (150)

cyclic regime reveal slight decreases in the tensile strength, but no effect on the strain capacity is observed.

The curves obtained from the cyclic tests show characteristic hystereses, from which it can be clearly recognised that the observed high strains are to a great extent due to non-elastic deformations (see strains at zero stress). Furthermore, the stiffness of the composite gradually decreases; that is, the inclination of the hysteresis curves with regard to the strain axis declines. The shapes of a number of chosen cycles are presented in Fig. 5 for two representative cyclic tests.

Table 3 gives values of the respective secant modulus of elasticity for several chosen strain levels. When the strain gradually increases from 0.5% to 2.0%, a very pronounced decrease in this characteristic, indeed by a factor of approximately 2.5, can be observed. At higher strain levels the decrease in stiffness continues.

Last but not least, the crack patterns observed on the specimens' surfaces were evaluated by visual inspection. For this purpose, the crack development during each particular test was monitored by a high-resolution digital camera. Table 4 gives a statistical evaluation of the crack number, average crack width and maximum crack width observed in both types of tests at the strain levels of 0.5%, 1.0%, and 2.0%, respectively. The statistical evaluation given is related to the specimens' crack patterns in the loaded state only.

Generally the number of cracks increases with increasing strain level while the average and maximum crack widths become slightly larger. The values do not differ much with regard to the loading regime. The deformation-controlled cyclic tests provided on average fewer cracks with slightly larger crack openings in comparison with the tests conducted under the monotonic regime. More testing is needed in order to prove whether this difference is statistically significant. Fig. 6 gives the representative crack patterns monitored on one of the specimens tested in the deformation-controlled monotonic loading regime at several strain levels.

After unloading in the cyclic regime, crack patterns observed at the residual strain levels of 0.5%, 1.0% and 2.0%, respectively, revealed a slightly higher number of cracks due to the higher strain level reached in loaded state before unloading. The crack widths were obviously lower due to the unloading.

Table 4
Statistical evaluation of crack system on specimens' surfaces as observed in uniaxial tension tests.

Type of loading	Strain ε (%)	Number of cracks n (−)	Average crack width w (mm)	Maximum crack width w_{max} (mm)
		Average value (standard deviation)		
Monotonic	0.5	4 (−)[a]	0.03 (−)[a]	0.05 (−)[a]
	1.0	8 (2)	0.05 (0.00)	0.08 (0.01)
	2.0	12 (3)	0.07 (0.01)	0.13 (0.06)
Cyclic	0.5	4 (0)	0.05 (0.01)	0.06 (0.01)
	1.0	6 (1)	0.07 (0.01)	0.11 (0.06)
	2.0	9 (1)	0.09 (0.01)	0.15 (0.05)

[a] Only one measurement was performed.

4. Tensile tests on single fibres

4.1. Fibre characteristics, test setup

Twelve millimeter-long PVA fibres (Kuraray Co., Ltd., Kuralon K-II REC15) with a specified diameter of 40 μm were used as dispersed reinforcement for the SHCC investigated. Single fibres were tested in order to provide their basic mechanical characteristics which are essential for the material modelling. Moreover, additional information was expected from this tension testing with respect to the behaviour of fibre under cyclic loading. Still further, due to the specific test setup the results should help in interpreting the results obtained in the subsequent fibre pullout tests.

Fibre was glued between two mounting plates of the testing machine using a commercially available adhesive for metals and plastic materials. Fig. 7 gives further details of the setup in use. Deformations were monitored both by measuring the machine cross head displacement and by evaluating the images obtained with a high-resolution camera with a macro-object lens. The photographs taken during the tests and evaluated using special software were used to find out if there is possibly an influence of imperfect gluing or the deformation of the load cell itself on the results observed. Fibre free length (between the glued ends) to be tested was set to 5 mm.

Similarly to the tensile tests on the dumbbell specimens, deformation-controlled monotonic and cyclic loading regimes were

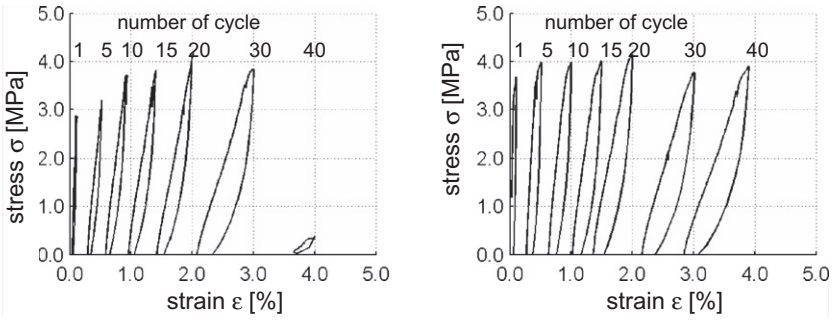

Fig. 5. Representative shapes of particular cyclic loops.

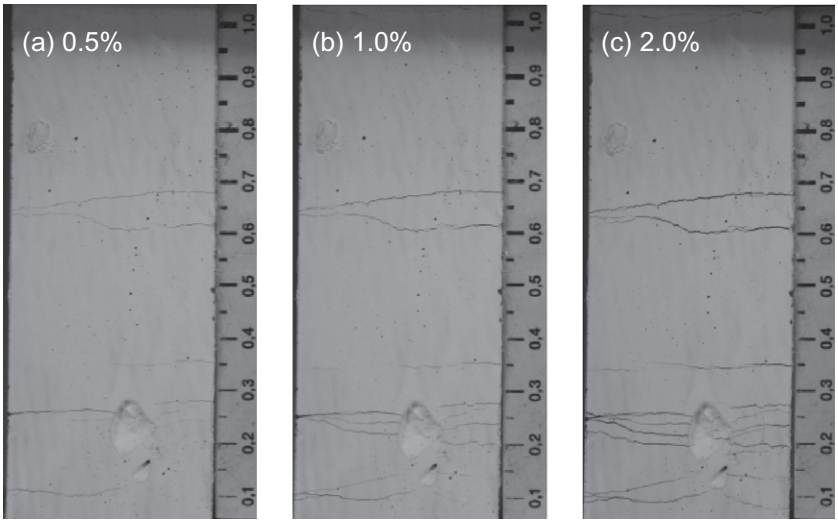

Fig. 6. Representative crack patterns on the surface of an SHCC specimen in the loaded state (monotonic deformation-controlled loading regime) at strain levels of: (a) 0.5%, (b) 1.0%, and (c) 2.0%.

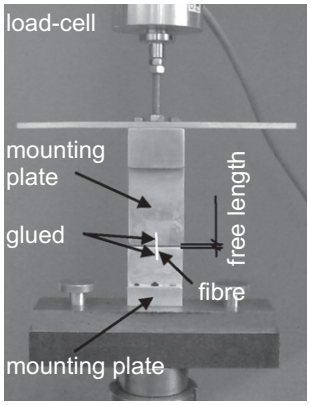

Fig. 7. Setup used for fibre testing, load cell and mounting plates of testing device.

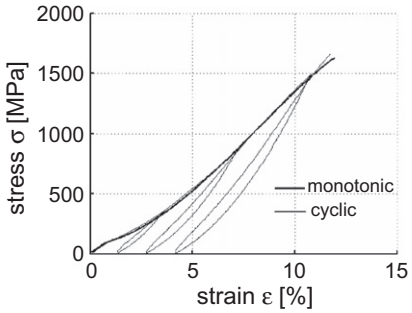

Fig. 8. Characteristic stress–strain behaviour of a single fibre under monotonic and cyclic deformation-controlled loading regimes.

applied. The loading rate was 0.01 mm/s. A strain increment of 5%, related to the initial free length, was prescribed for each cycle of the cyclic tests. Three tests were performed under each loading regime.

4.2. Results of the tension tests on single fibres

A free fibre length of 5 mm was used in testing, which is relevant as a reference for the fibre pullout tests; see Section 5. Table 5 gives the average fibre characteristics obtained.

In general, the response of single fibres is nearly linear; however, after unloading a considerable irreversible strain can be observed (Fig. 8). This strain component amounts to 41% of the total strain. Fig. 8 gives the comparison of the representative single-fibre behaviour under deformation-controlled monotonic and cyclic loading regimes. It should be mentioned here that as presented in Section 6, optical observations of single fibres revealed that the fibre diameter is lower than that claimed by the producer. The stress values used for Fig. 8 were calculated using the correct diameter. Furthermore, the strain values were calculated under consideration of the real free length, which can differ from the given free length due to the imperfect gluing procedure. In addition, the deformation of the load cell was subtracted from the results obtained. For these reasons, the cyclic loops shown in Fig. 8 appear at different strain levels than those predicted.

Additionally, single fibres were tested in a load-controlled creep regime. The time-dependent deformation components were found to be insignificant and, hence, negligible.

Table 5
Measured characteristics of single fibres.

Free length l (mm)	Tensile strength σ (MPa)	Strain capacity ε (%)	Secant modulus E (GPa)	Irreversible strain component δ (%)
5	1620	11	15	41

5. Single-fibre pullout tests

5.1. Specimen description, casting, curing, test setup

The test setup was based on the approach presented by Kabele et al. [12]. The fibre was inserted into a hollow medical cannula with a blunt tip. The position of the fibre was then fixed with wax when the desired embedment length was attained. The embedded length was subsequently measured by using images made by a high-resolution camera. The constant diameter of the cannula was used as a reference "scale". Finally, the frame with a number of cannulae was fixed to the mould, and the SHCC matrix without fibres was added until the ends of cannulae lay 1 mm beneath the matrix surface. This arrangement prevented possible

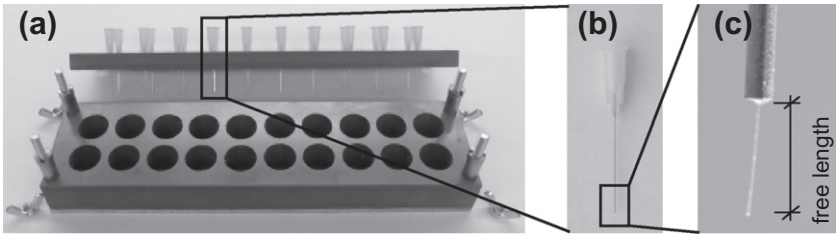

Fig. 9. Production of specimens for the fibre pullout tests: (a) mould and cannula frame, (b) single cannula, (c) detail of a fixed fibre.

influence on the bond properties by carbonation. Fig. 9 shows further details of the specimen preparation.

It should be mentioned here that the arrangement described does not enable testing the effect of fibre declination from the axis perpendicular to the matrix surface on its pullout performance. Thus, such tests were not performed in this study. For the purpose of subsequent modelling, the effect of fibre inclination will be considered using an approach from the literature in the second part of this paper which is dedicated to modelling.

The mould was stored for 2 days in a climate room, subsequently sealed with a polymer foil, and stored for 26 days at room temperature before de-moulding. Since the bond between wax and fibre was much weaker than the bond between fibre and matrix, the specimens were not damaged. The test setup was similar to that used for the fibre testing (cf. Fig. 7); however, the bottom mounting plate was replaced by a clamping device. After clamping the specimen the fibre was glued to the upper mounting plate in the same way as already described in the fibre testing.

The experimental program included deformation-controlled monotonic and cyclic tests. The loading rate was again 0.01 mm/s, and the displacement increment of 0.1 mm was prescribed in each cycle. The fibres' embedded lengths were varied between 1 and 6 mm in increments of 0.5 mm. The free fibre length (between the embedded and the glued parts) was 5 mm as in the fibre tension tests. Five pullout tests were performed for each embedment length under monotonic regime; in total 55 tests were performed. In addition, 12 tests were performed under cyclic regime on specimens with different embedment lengths.

5.2. Results of the pullout tests

Typical force-to-deformation response consisted of an elastic portion (before full de-bonding) and a pullout portion, which was characterised by softening or hardening behaviour. Fibre failures could be observed in individual tests at any stage. However, fibre failure after the de-bonding in the softening regime took place only due to pronounced damage of the fibre after minor local hardening. This scenario was very rare and is not taken into consideration in modelling material behaviour.

Fig. 10a shows the results obtained from pullout tests under monotonic loading. Responses in the individual tests vary significantly, even for fibres having similar embedded lengths. Furthermore, the evaluation of the results showed that the fibres fail at much lower stress levels in comparison to the fibre tensile strength; in fact the stress level at failure was on average approximately 25% of the average tensile strength value. In order to clarify the mechanisms behind these phenomena, optical investigations using Environmental Scanning Electron Microscope (ESEM) were performed; see Section 6.

Tables 6 and 7 present a statistical evaluation of the results obtained under a deformation-controlled, monotonic loading regime. Table 6 gives the number of fibres undergoing the particular failure or pullout scenarios as described above. No pronounced tendency with respect to fibre performance can be observed when the embedded length changes. Such an unexpected result can be related to the influence of pullout behaviour by specific arrangement of matrix constituents in the vicinity of the fibre and to the possible difference between the prescribed and actual fibre embedded

Table 6
Number of fibres failed or pulled out in particular scenarios.

Embedded length l (mm)	Number of fibre failures (–)		Number of fibres completely pulled out f (–)		Total number n (–)
	Before de-bonding	After hardening	After softening	After hardening	
1.0	2	1	2	0	5
1.5	2	1	2	0	5
2.0	0	2	3	0	5
2.5	0	0	5	0	5
3.0	0	1	3	1	5
3.5	0	1	2	2	5
4.0	1	1	3	0	5
4.5	0	2	2	1	5
5.0	2	2	1	0	5
5.5	0	2	3	0	5
6.0	0	3	2	0	5
Number n (–)	7	16	28	4	55

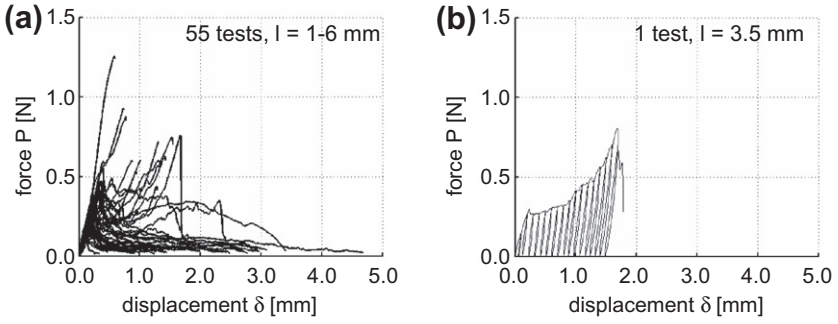

Fig. 10. Representative results of pullout tests: (a) under monotonic loading regime, and (b) under deformation-controlled, cyclic loading regime.

Table 7
Characterisation of pullout results.

Pullout scenario	Fibre failure before de-bonding		Fibre failure after hardening		Completed pullout after softening		Completed pullout after hardening	
Characteristic values	Min	Max	Min	Max	Min	Max	Min	Max
Displacement δ_0 (mm)	0.09	0.59	0.04	0.54	0.12	0.44	0.23	0.25
Force P_0 (N)	0.10	1.24	0.05	0.58	0.13	0.46	0.27	0.35
Displacement δ_h (mm)	–	–	0.05	1.54	–	–	0.25	1.93
Force P_h (N)	–	–	0.06	0.92	–	–	0.34	0.75
Displacement δ_u (mm)	–	–	–	–	0.33	4.68	0.54	3.40

lengths, as described in Section 6. In general, the highest number of fibres is fully de-bonded and pulled out of the matrix while showing softening behaviour (28 from 55, cf. Table 6). In contrast, fibres are markedly prone to failure either before de-bonding (7 from 55) or in the hardening regime after full de-bonding (16 from 55, cf. Table 6). Fibres fully pulled out of the matrix after the foregoing hardening are observed in several cases only (4 from 55).

Since no statistical relationships could be found to explain the results of the pullout tests, each defined fibre failure or pulling out scenario must be described independently for different fibre embedment lengths by the lower and upper limits of the experimentally obtained pullout displacements and forces. Table 7 gives the ranges for the different pullout scenarios used.

The pullout responses can be described by a number of characteristic values corresponding to specific points of the force–displacement diagram. The number of such points depends on the particular behaviour observed during the pullout test. Except for the origin of the coordinates (first point), the second two characteristic values of each pullout response are the displacement and the force at the point where fibres either break or fully de-bond. Such point is associated with the global maximum in force (fibre broken before de-bonding or de-bonded and pulled out in softening regime) or with the first local maximum in force (fibre broken or pulled out after full de-bonding in hardening regime), see Fig. 10. This pair of values, defining the second characteristic point, is referred using the index "0" in Table 7. The third pair of characteristic values gives the ultimate displacement and force reached (both marked with index "*h*"). This third point is relevant for fibres being broken or pulled out after exhibiting slip hardening and is associated with the global maximum in force of the pullout responses. The last characteristic value is the displacement at a force equal to 0 (referred with index "*u*") which is relevant for fibres having been fully pulled out after softening or hardening. These values define the fourth and last characteristic point.

The tests performed under cyclic loading revealed results consistent with respect to the shape and inclination of unloading and reloading branches. Thus, only one representative force–displacement curve is presented in this paper, see Fig. 10b. These tests did not reveal any pronounced effect of the loading regime on the pullout behaviour. The shape of the cyclic loops was not influenced by the scenario of subsequent failure, i.e. fibre breakage on or after hardening, or fibre pullout after hardening or during the softening process. It could be concluded that the shape of the individual unloading–reloading loops was only dependent on the force prior to unloading.

Because pullout deformation was found to be irreversible, the shape of unloading and reloading branches during pullout testing is primarily related to the deformation of the fibre within its initial free length and the length of the region where a partial de-bonding of the fibre from the matrix occurred. Deformation of the fibre itself is, however, quite low in comparison to the pullout displacement developed during the test.

In the region where de-bonding occurred, the fibre-deformation behaviour is influenced by the friction between fibre and matrix. This phenomenon can also be time-dependent; see Boshoff et al. [13]. However, the time dependency of the pullout process is neglected in this investigation because the creep contribution is insignificant due to the relatively short duration of the tests.

Due to the "imperfect" pullout setup arrangement, the results obtained are influenced by the deformation of fibre free length between the point where it exits the matrix and the glued fibre end. Since no considerable free length is involved in the cracking of SHCC in the hardening regime, this deformation component has to be subtracted from the results in order to obtain a representative description of single-fibre pullout behaviour to be used further in modelling.

6. Optical investigations

Optical investigations of the microstructure were performed on the cracked SHCC surfaces and on pullout specimens after mechanical testing by using ESEM. The purpose of these observations was to clarify the pronounced differences in pullout behaviour as observed in the experiments. Matrix cylinders used in the pullout testing were split into two pieces in order to gain access to the embedded fibre and to the fibre–matrix interface. Additionally, the fibres pulled out of the matrix were investigated as well. As a reference with respect to fibres partly damaged during the pullout process, the undamaged fibres were studied.

In considering the causes of the pronounced scattering of the pullout test results, it should be stressed that the structure of SHCC cannot be considered as homogenous at this level of observation. Fig. 11a, which was obtained by visual investigation of a cracked SHCC surface, shows that the fibre diameter is comparable to the size of the sand particles as well as those of the fly ash. Therefore, the results of each pullout test depend on the particular coarse microstructure in the vicinity of the fibre. Since the sand and fly ash particles are stiffer than the fibre, contact during pulling-out process will result in fibre damage and subsequently in a decrease in the load at failure.

Fig. 11b, developed from an investigation of a split pullout specimen, indicates that the same dependence of fibre-pullout performance on particular properties of the matrix in fibre vicinity exists also in the pullout tests. Furthermore, from this example it can be clearly seen that the nominal embedded length of the fibre can differ significantly from the length really in contact with the matrix due to local imperfections in the matrix, such as air voids. Such imperfections can be most probably related to the insufficient compaction of the matrix around the fibre. Since the contact area is a crucial parameter, this difference may play an important role. Apart from the local damage caused by contact with the surrounding particles, a stress concentration in the fibre due to local loss of contact with the matrix, see Fig. 12a, is a possible explanation for early fibre failure during the pullout process.

To initiate the pullout process, the force of the chemical bond must be exceeded. Depending on local interface properties, the resistance to pullout can decrease together with decreasing friction

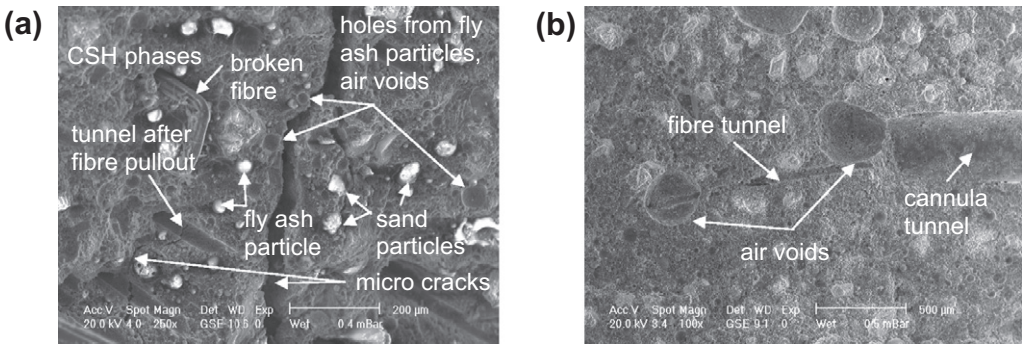

Fig. 11. Optical investigations of SHCC microstructure: (a) cracking surface indicating the importance of material heterogeneity, and (b) split pullout specimen with air voids changing the effective embedment length.

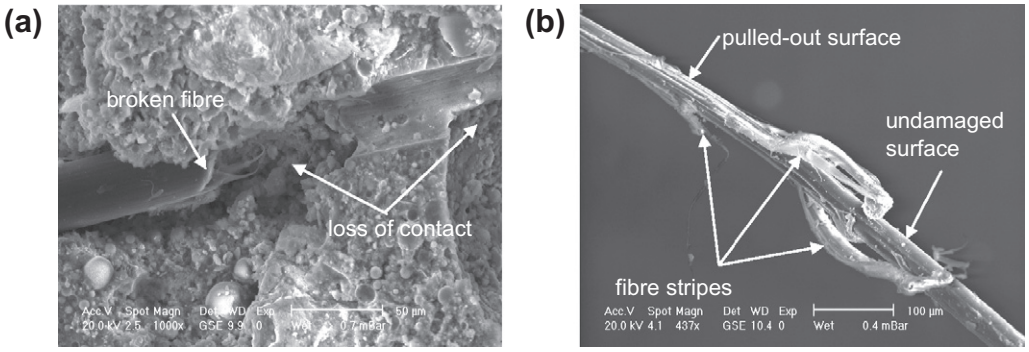

Fig. 12. Optical investigation of SHCC microstructure: (a) split pullout specimen indicating possible failure of the fibre as result of stress concentration due to the loss of the contact with the matrix, and (b) pulled-out fibre damaged by friction with the matrix.

surface as the result of the gradual pullout. Often, however, the matrix damages the fibre surface, subsequently leading to an increase in the pullout resistance. A few pulled-out fibres were investigated in order to verify this assumption. Fig. 12b shows a typical view of the fibre damaged due to the friction with the matrix after the pullout.

In order to determine the exact diameter of PVA fibre, eight fibres were measured at eight different cross-sections chosen at different locations over the fibre length. The average diameter obtained was 37.1 μm (i.e. slightly lower than that specified by the manufacturer), while the standard deviation was 2.1 μm. Diameters varied significantly between individual fibres, but the variation along the length of any particular fibre was very low.

7. Summary and outlook

The results of the experimental investigation and the conclusions drawn can be summarised as follows.

Uniaxial tensile tests under deformation-controlled monotonic and cyclic loading regimes provided detailed characteristics of the specific behaviour of SHCC. The results observed did not show any pronounced effect of loading conditions on material performance. The analysis of the hystereses of the stress–strain curves showed a pronounced decrease in the material stiffness with an increasing number of loading cycles; the hysteresis loops became rounder as well. The hystereses further revealed a considerable partial inelastic deformation in every loop. The number of cracks as well as their individual widths as observed on the specimen's surfaces did not vary much for the two loading regimes investigated. The number of cracks developed gradually in relation to the strain level reached.

The behaviour of a single PVA fibre can be considered as linear elastic–plastic. Detailed characteristics of material performance were derived. It was concluded that the components of irreversible deformation cannot be neglected. Fibre creep can be however considered insignificant.

The pullout tests showed that their results can vary significantly. Four main pullout scenarios were described in detail, and a statistical evaluation was presented. When the chemical bond is exceeded and complete fibre de-bonding occurs, the pullout process becomes irreversible. Furthermore, the pullout displacements are much higher than the fibre deformations. Therefore, the pullout behaviour is of high importance for the overall tensile performance of SHCC.

The microscopic investigations showed that the material structure cannot be considered to be homogeneous at the microscopic level of observation. The size of the aggregate and fly ash particles used in SHCC cannot be neglected when single-fibre pullout is considered. Because of this the pullout behaviour is characterised by the limiting values of the characteristic points in the measured curves, as observed in the experiments.

Current information on the behaviour of the SHCC under investigation at different levels of observation will be further used for the development of constitutive relations. This is the subject of the second part of this paper.

References

[1] Fischer G, Li VC editors. International RILEM Workshop on HPFRCC in structural applications. Honolulu: RILEM Publications S.A.R.L., PRO 49; 2005.
[2] Mechtcherine V editor. Ultra-ductile concrete with short fibres – development, testing, applications. Stuttgart: Ibidem-Verlag; 2005.
[3] Mechtcherine V. Testing behaviour of strain hardening cement-based composites in tension – summary of recent research. In: Reinhardt H-W,

Naaman editor. ARILEM-symposium on high-performance fibre reinforced cementitious composites HPFRCC5. RILEM PRO 53; 2007. p. 13–22.
[4] Fukuyama H, Haruhiko S, Yang I. HPFRCC damper for structural control. In: Proceedings of the JCI international workshop on ductile fiber reinforced cementitious composites (DFRCC), Takayama (Japan): Japan Concrete Institute; 2002. p. 219–28.
[5] Douglas KS, Billington SL. Rate-dependence in high-performance fiber-reinforced cement-based composites for seismic applications. In: Fischer G, Li VC editors. International RILEM workshop on HPFRCC in structural applications, Honolulu, May 2005. RILEM Publications S.A.R.L., PRO 49; 2006. p. 17–26.
[6] Mechtcherine V, Jun P. Stress–strain behaviour of strain-hardening cement-based composites (SHCC) under repeated tensile loading. In: Carpinteri, A. et al. (Hrgb.) editor. Fracture mechanics of concrete structures. London: Taylor & Francis; 2007. p. 1441–8.
[7] Jun P, Mechtcherine V. Experimental investigation on the behaviour of strain-hardening cement-based composites (SHCC) on different levels of observation. International Workshop NMMF 2007. Wuppertal (Germany): Aedificatio Publishers; 2007. p. 137–50.
[8] Jun P, Mechtcherine V. Deformation behaviour of cracked strain-hardening cement-based composites (SHCC) under sustained and repeated tensile loading. In: Tanabe, T. et al. editor. Proceedings of 8th int conference on creep, shrinkage and durability of concrete structure, CONCREEP 8. Ise-Shima, London (Japan): Taylor & Francis Group; 2008. p. 487–93.
[9] Li VC. From micromechanics to structural engineering – the design of cementitious composites for civil engineering applications. JSCE J Struct Mech Earthquake Eng 1993;10(2):37–48.
[10] Mechtcherine V, Schulze J. Ultra-ductile concrete – material design concept and testing. In: V. Mechtcherine editor. Ultra-ductile concrete with short fibres – development, testing, applications. Stuttgart: Ibidem-Verlag; 2005. p. 11–36.
[11] Mechtcherine V, Schulze J. Testing the behaviour of strain hardening cementitious composites in tension. In: Fischer G, Li VC editors. Int RILEM Workshop on HPFRCC in structural applications, Honolulu, May 2005. RILEM Publications S.A.R.L., PRO 49; 2006. p. 37–46.
[12] Kabele P, Novák L, Němeček J, Kopecký L. Effects of chemical exposure on bond between synthetic fiber and cementitious matrix. Textile reinforced concrete – proceedings of the 1st international RILEM conference. Cachan: RILEM Publications; 2006. p. 91–9 [ISBN 2-912143-97-7].
[13] Boshoff WP, Mechtcherine V, van Zijl GPAG. Characterising the time-dependent behaviour on the single fibre level of SHCC – part 1: mechanism of fibre pullout creep. Cem Concr Res 2009;39:779–86.